INT 174/91 December 1991

MULTI-CHANNEL INTERFEROMETER FRINGE COUNTING USING A NEURAL NETWORK

J.B. Lister and C. Nieswand

MULTI-CHANNEL INTERFEROMETER FRINGE COUNTING USING A NEURAL NETWORK

J.B. Lister and C. Nieswand
Centre de Recherches en Physique des Plasmas
Association Euratom - Confédération Suisse
Ecole Polytechnique Fédérale de Lausanne
21, Av. des Bains, CH-1007 Lausanne, Switzerland

1) INTRODUCTION

The "loss" of fringes in an interferometer is a fundamental problem since the physically observable function of the total phase shift ψ is $\phi = \text{Mod}\ (\psi, 2\pi)$. In order to construct ψ from ϕ we obviously require additional information. The only sources of information available are the spatial correlations between $\phi(x_i,t_k)$ and $\phi(x_j,t_k)$ where $x_i\, x_j$ represent different integration paths or the time-correlations between $\phi(x_i,t_k)$ and $\phi(x_i,t_l)$. The 2-wavelength interferometer providing $\phi = \text{Mod}(\psi(\lambda),2\pi)$ is an elegant solution which we assume is not implemented, or at least not implemented for all chords.

The conventional solution in a multi-channel interferometer is a multiplicity of the single-channel fringe jump algorithm which selects ψ on the criterion of minimum change in ψ between successive samplings, as implemented on TCA. This algorithm is simply coded for real-time evaluation of $\psi = \phi + n \bullet 2\pi$ given the estimated value of n.

Unfortunately, $\psi(t)$ can be discontinuous in time, on the timescale of a fringe-counting algorithm, for example following the injection of a pellet or an L-H transition. In such cases we are in trouble.

One way out is to work back from the end of the discharge. This is unreliable in general due to a frequent second fringe loss at the small plasma current extinction disruption at this end of the plasma pulse. It is

also irrelevant if we inject more than one pellet, and unusable for real-time control.

What is normally done is to inspect the chord integrals of the multi-channel interferometer, and perform a visual constraint of spatial coherence, and guesstimate the fringe counter corrections.

During discussion at JET, it was proposed that we look at a Neural Network as a way of providing an automatable algorithm using spatial coherence as a method of determining the fringe counts of a multi-channel interferometer.

This note describes the tests performed on TCA data to evaluate the usefulness of this method for JET.

2) THE TCA PROBLEM

TCA was equipped with a 4-channel methyl-iodide laser interferometer, $\lambda = 447\ \mu m$, Fig. 1. The size and densities of the TCA plasma limited us to approximately 5 fringes. We possess a database of 1000 selected discharges in which, as a result of human endeavour, we assume there to be no fringe errors.

3) THE JET PROBLEM

JET has 6 chords with up to 60 fringes, Fig. 2. This large number will be a problem because the percentage error caused by a fringe error will be smaller.

4) THE NEURAL NETWORK

We considered that the most productive approach would be the identification by a Multi-Layer Perception (MLP) of the fringe counter error. The data input for one time sample of the 4 channels i = 1..4 would be:

$$\psi_i = \phi_i + 2\pi\, n_i + \varepsilon_i 2\pi$$

where ε_i is the error in the input data. The required output is the vector constructed out of the ε_i. This approach was preferred due to its simple implementation as a fringe-counter corrector, if there is an existing fringe-counter, or as a full fringe counter. The latter functions, by starting the discharge with $n_i = 0$, and evaluating $n_i = n_i + \varepsilon_i$ for each iteration. By successive interation we would expect that entering the MLP with

$$\psi_i = \phi_i + 2\pi\, n_i + \varepsilon_i 2\pi - \varepsilon_i 2\pi$$

as the new data, we would obtain $\varepsilon_i = 0$.

The MLP was trained as a batch cycle, as described in detail in LRP 389/90, using the Generalized Adaptive Recipe.

The input and output data were always re-normalized to the full range ±1.0.

Task 1 - 1 positive fringe jump

One of the 4 TCA chords was perturbed by +1 fringe on 40% of the 1000 examples. The MLP was trained with 10 hidden neurons, and convergence was obtained in 900 iterations.

The result obtained was a 100% separation between cases with and without fringe-jumps.

Task 2 - 1 fringe jump of ±1 fringe

One of the 4 chords was perturbed in 50% of the data by either +1 or -1 fringes (50:50). Training took 3600 iterations and separation was perfect. Figure 3 shows a histrogram of the output data for the 4 channels. The outermost channels (1 and 4) are perfectly separable. The innermost channels (2 and 3) are already less well separated.

These 2 test cases assume that there will only be one fringe error. The stability of this one-by-one correction of the fringe error is by no means obvious, especially after a pellet is injected.

Task 3 - One fringe jump of 1/4 fringe

We re-quantised the data, assuming 20 fringes on TCA, and allowed a single fringe-jump. This is equivalent to permitting a 1/4 fringe jump for the TCA discharges. Again, we polluted half of the database and trained for 48'000 iterations. The trained data set now contains errors after learning, 3, 7, 7 and 3 errors out of 500 cases for the 4 channels respectively. We have, therefore, identified cases in which the true data modified by 1/4 fringe look "more reasonable" and cases which the 1/4 fringe jump did not look "unreasonable".

Task 4 - idem, full data

In Task 3 we effectively removed data from the good samples when we polluted them. In this Task we accepted all good discharges, and polluted each channel twice, once by 1/4 fringe and once by -1/4 fringe, giving a total of 9 examples, 1 correct and 8 with errors, for each TCA discharge. The 9000 examples were the trained. (For the case of ±1 fringe errors the separation was perfect). The separation is shown in Fig. 4 in which we see that there is no clear separation between zero and 1/4 fringe errors, even for the outer channels.

We believe that the discharges are well distributed in the input-space. An imperfect separation can result from two causes:

- noise on the input data
- variation in the input data

The first problem is considered irrelevant at the level of ±1/4 fringe. The lack of separation is therefore genuine, and corresponds to the "acceptable" or "genuine" data having a width of the order of 1/4 fringe in the input-space itself. Put more crudely, we are presenting the same data twice, once called "good" and once called "bad" and the MLP is just confused.

Task 5 - idem, more channels

To test this conclusion, we generated a new TCA data set with 7 FIR chords forcing a smooth curve through the 4 physically measured points, and generating 3 new interpolated "chords".

We now create 15 examples per discharge. Training on ±1 fringe jump gave us total separation. Training on ±1/4 fringe separation gave us excellent results. Figure 5 shows a histogram of the output estimates showing the almost perfect separation on all channels.

Change in algorithm

Since we assume a fringe jump $\varepsilon_i = 1$ if the output $i > 0.5$, and $\varepsilon_i = -1$, if the output $i < -0.5$, we do not need to force the fringe error to be exactly normalized, just that it be $\lesssim \pm 0.5$. The learning algorithm was modified to take this into account in what follows.

Retraining the data of Task 4 gave slightly improved results. Figure 6 shows the distributions of the predicted error (vertical axis) against the number of fringes (normalised to [+1, -1] for each chord separately). The horizontal lines show the fringe-counter decision boundary showing where confusion can (and will) arise. This represented our best separation using the 4 input channels.

Task 6 - Include $\beta + li/2$ and R_o as input data. We restricted ourselves to the case with 4 TCA channels and ±1/4 fringe errors. The improvements obtained were not dramatic.

Task 7 - Implementation of the Fringe Counter

In spite of the marginality of the success with 4 channels, we implemented the fringe-counter algorithm on raw TCA data. The fringe counter was incremented/decremented on the channel which showed the greatest error. The corrected data were then offered to the fringe counter for further correction.

A new problem is then encountered - runaway fringe errors - when the updated input signals suggest a further increment/decrement on the same channel. This seemed to occur when the input data left the learning volume of the input space, and a cut must be provided here.

Notwithstanding this difficulty, we obtained TCA discharges with injection of a pellet, which were mostly correctly fringe-counted by our algorithm. Figure 7 shows an example of a reconstruction.

5) CONCLUSIONS

This work has brought to light several important points:

- The use of only spatial properties of the interferometry data allows reconstruction of the fringe-count even after fringe-loss. There is no memory in the algorithm.

- The spatial information is inadequate given 4 chords and 20 fringes maximum density.

- Given 7 chords, the information provides a much better "vote" on the fringe-jumps.

- Adding extra equilibrium information is structurally straightforward, as we do not need to know how to use it.

If a multi-channel interferometer with enough cords is constructed for TCV, this algorithm can either be used to verify the temporal fringe-counter or as the primary fringe-counter.

If JET considers the method to be of interest, the exercise can be repeated on JET data. The aim would be to determine whether the Neural Network can recover the errors in the current algorithm, rather than do all the fringe-counting. (See Annex A)

Addendum:

We have not looked into the link between the Thomson n_e-profile and the interferometer, due to the lack of TCA data.

Annex A JET data test

The exercise can be repeated on JET data to determine the applicability of the method.

What is required is a file (Mac/PC) with an ASCII listing of a wide JET database containing for each entry:

- No. of fringes for each channel
- Current Centroid position
- External ($R > R_0$) last surface position
- Internal ($R < R_0$) last surface position
- $\beta + li/2$
- Triangularity

On completion of the learning, the same data can be used to create an "unseen" test sample.

FIG 2.

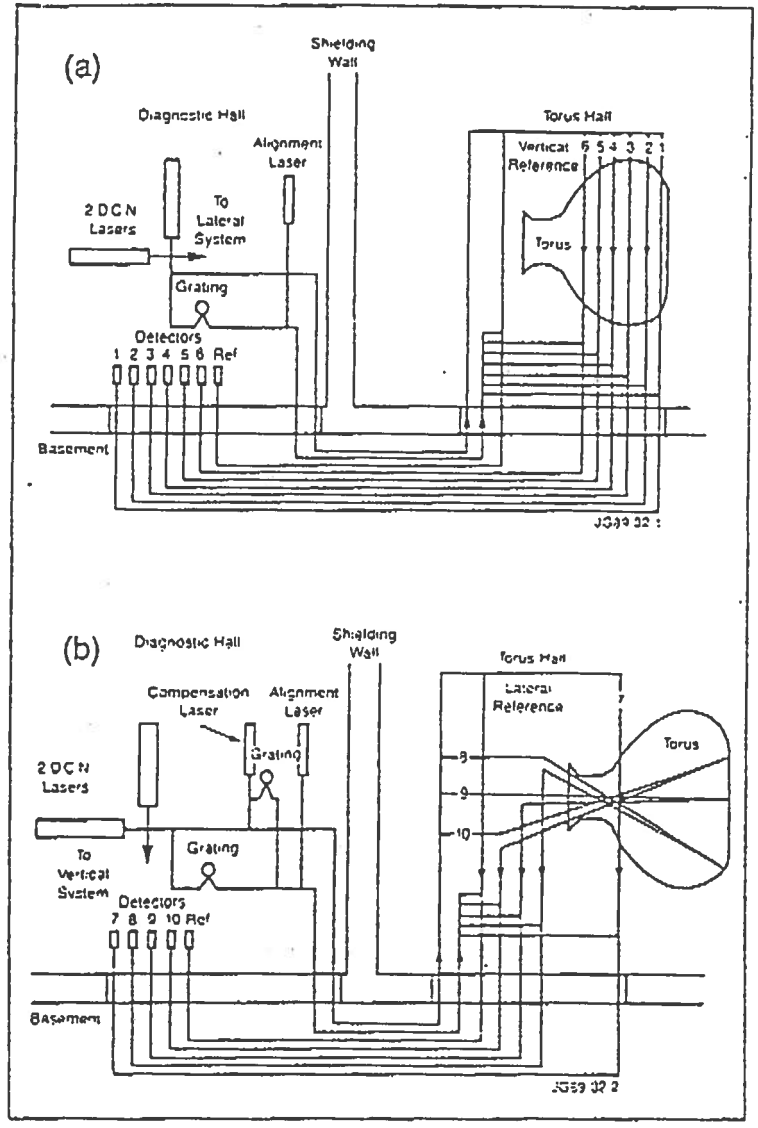

Fig. 1 Schematic view of the FIR Interferometer System
(a) Vertical probing (b) Lateral probing

FIG 1.

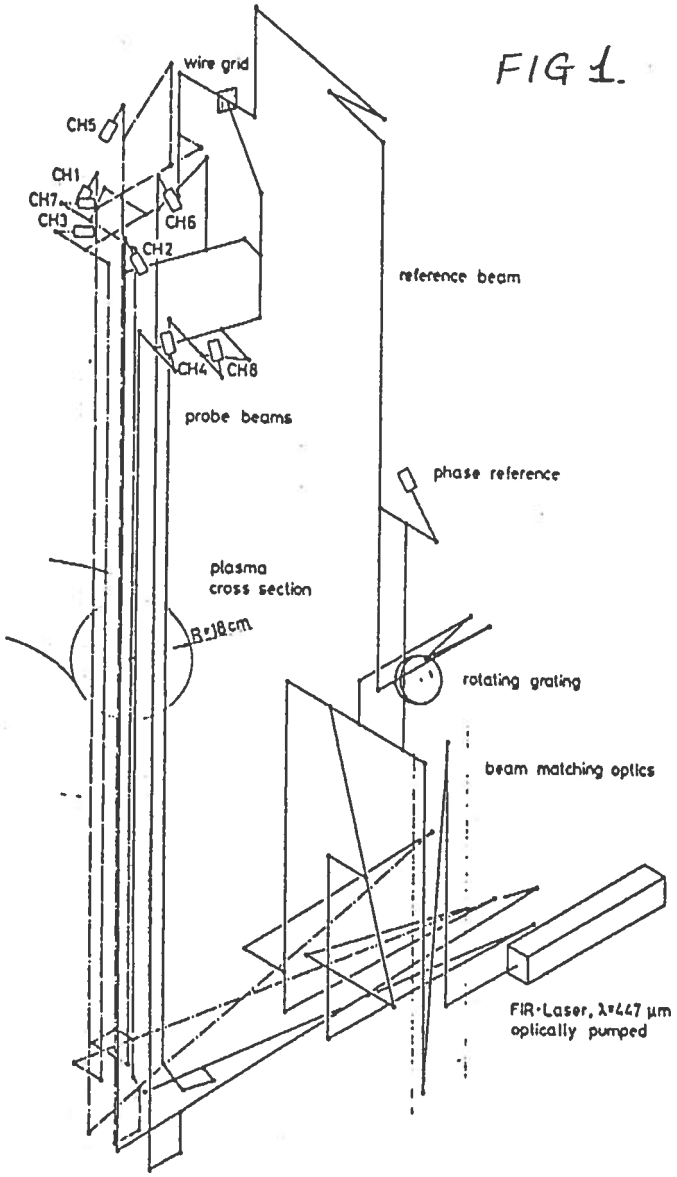

FIG 3.

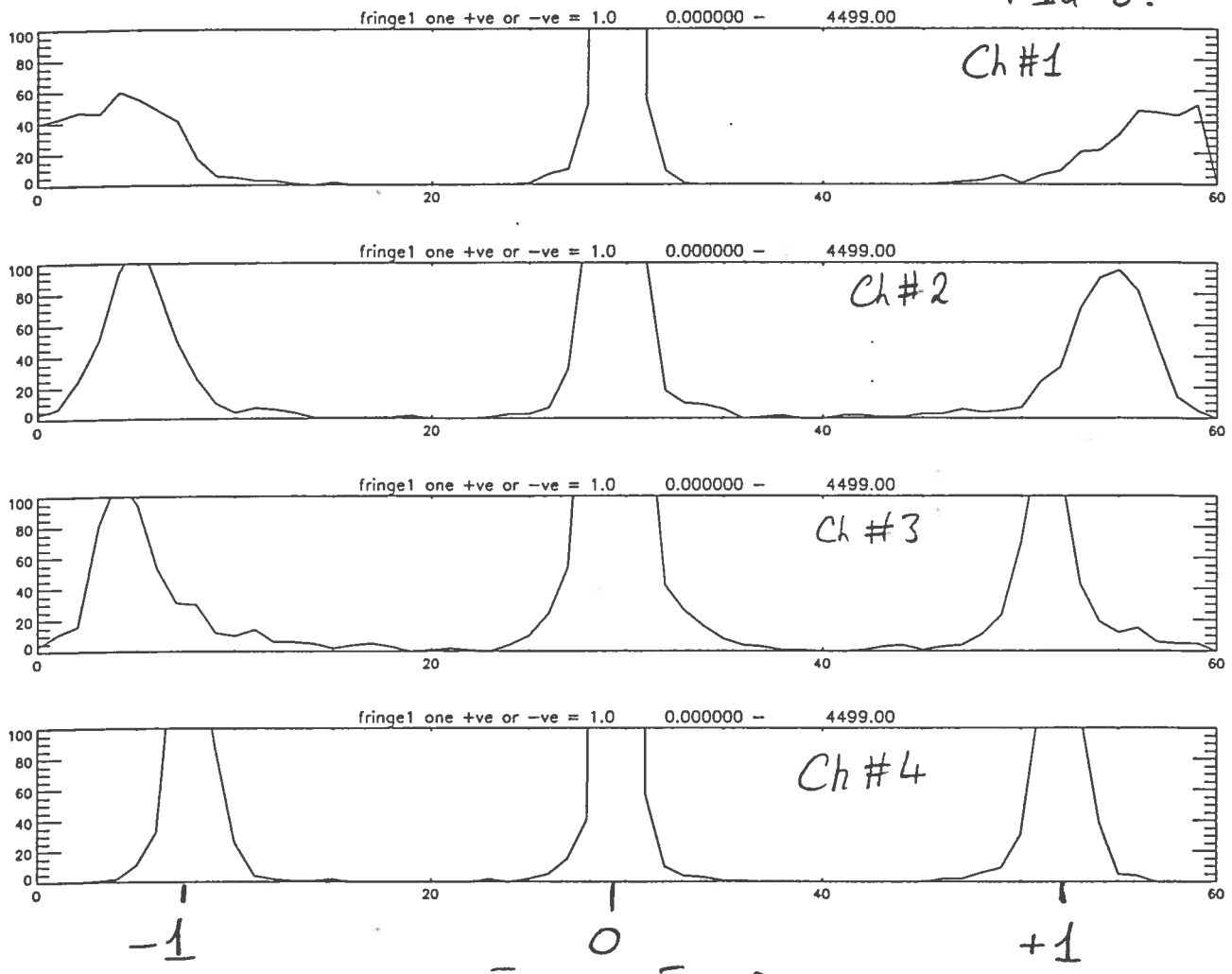

Fringe Error.

FIG 4

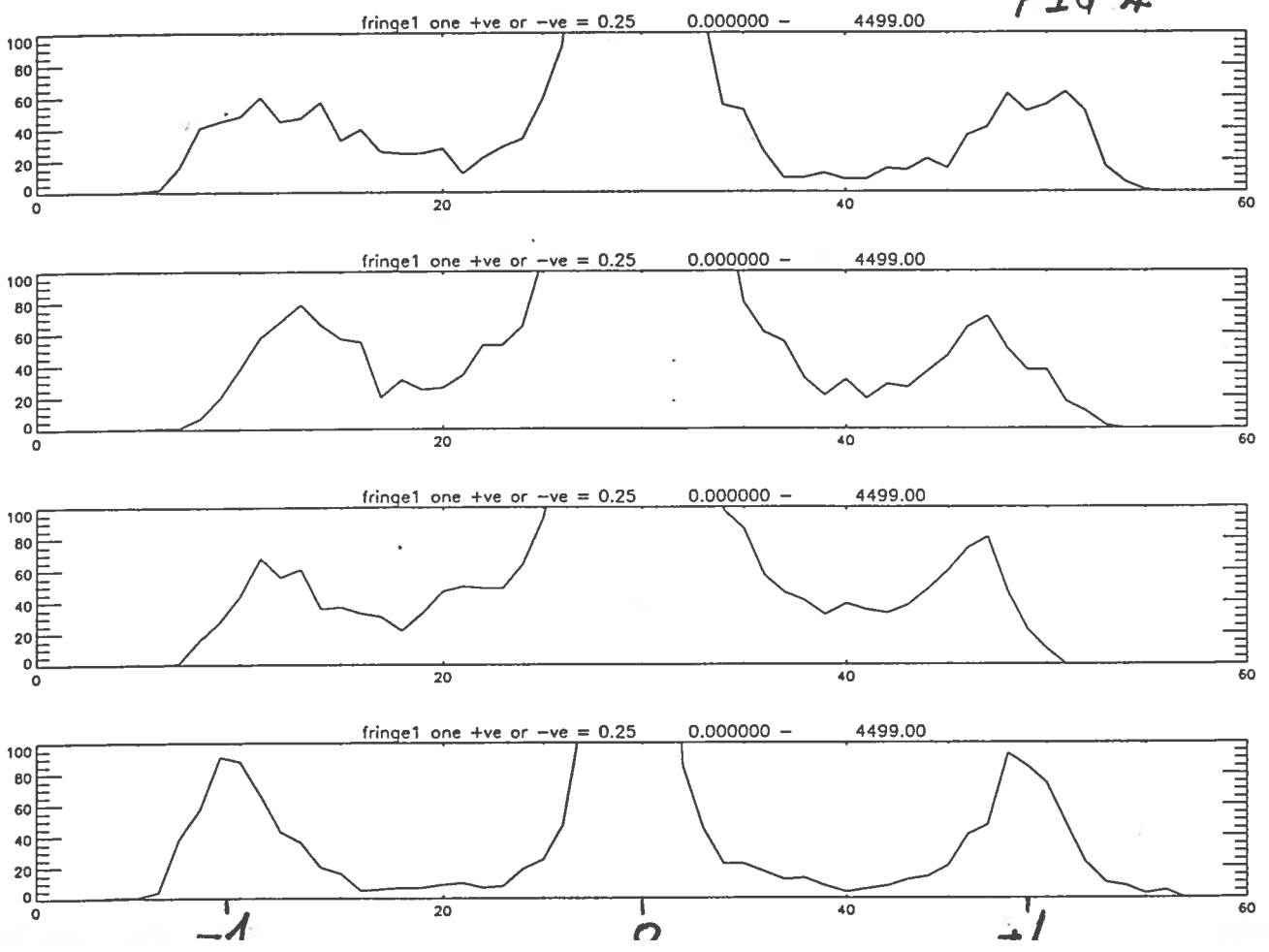

FIG 5.

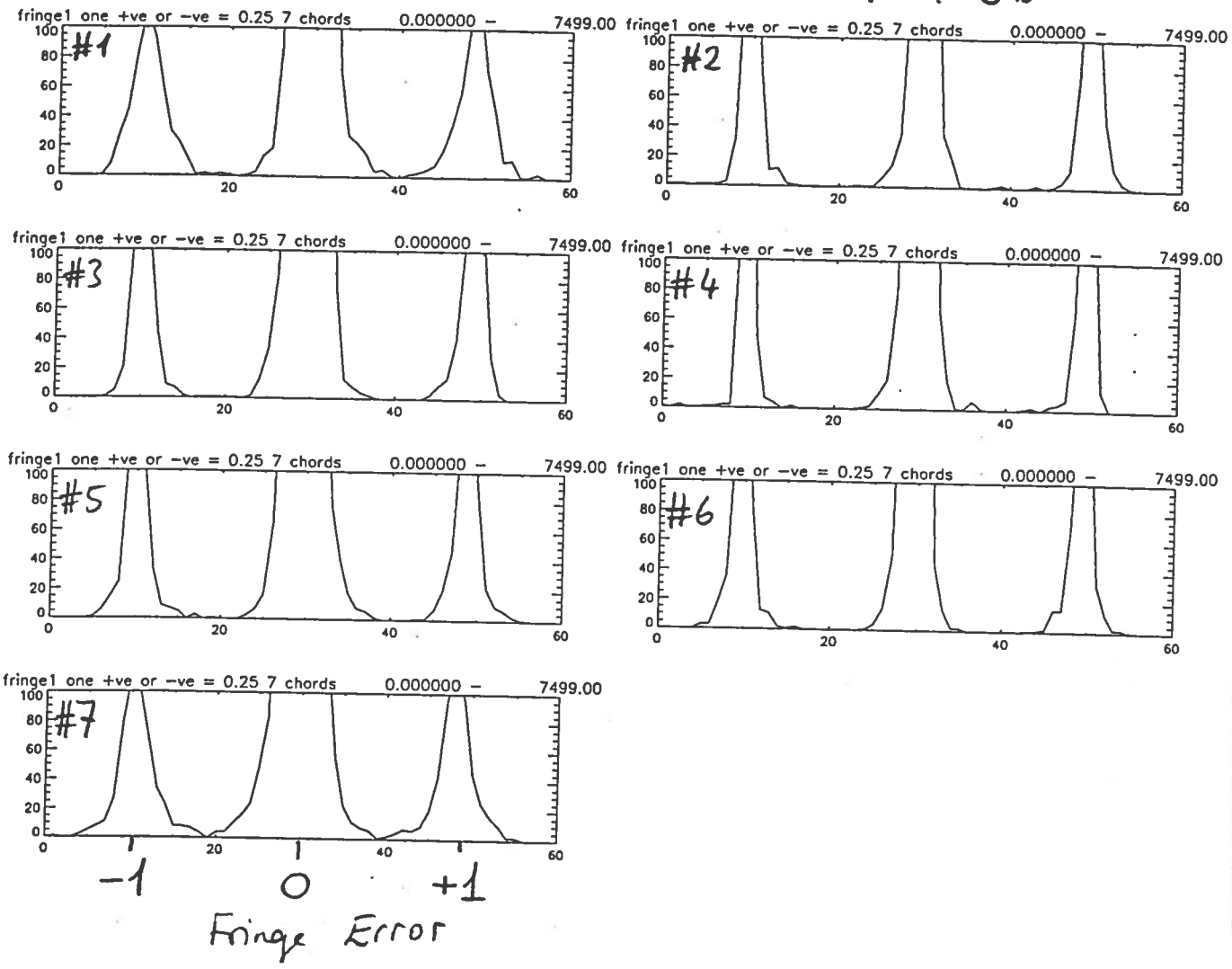
fringe1 one +ve or −ve = 0.25 7 chords 0.000000 − 7499.00
#1
#2
#3
#4
#5
#6
#7
−1 0 +1
Fringe Error

FIG 6.

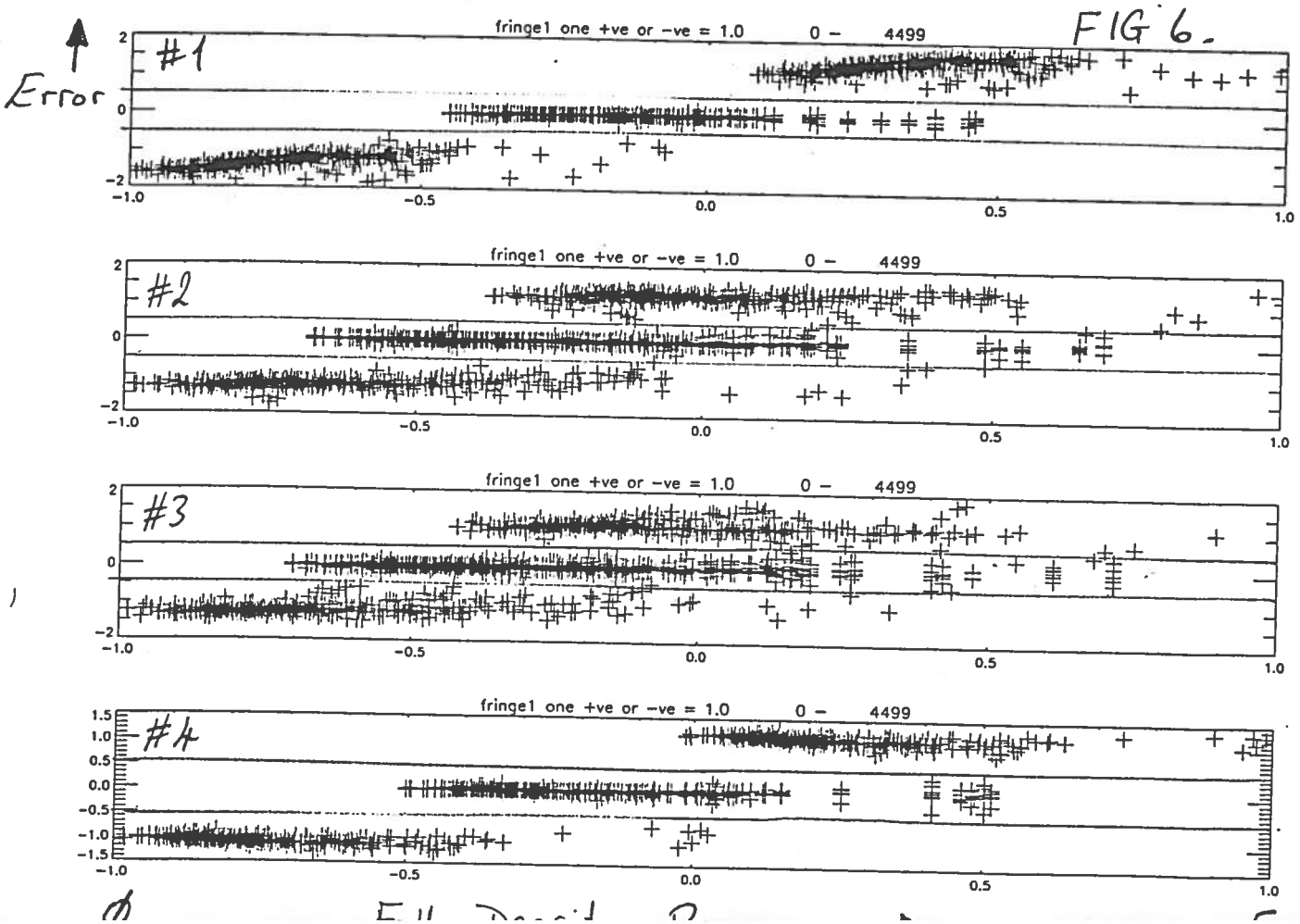
Error
fringe1 one +ve or −ve = 1.0 0 − 4499
#1
#2
#3
#4

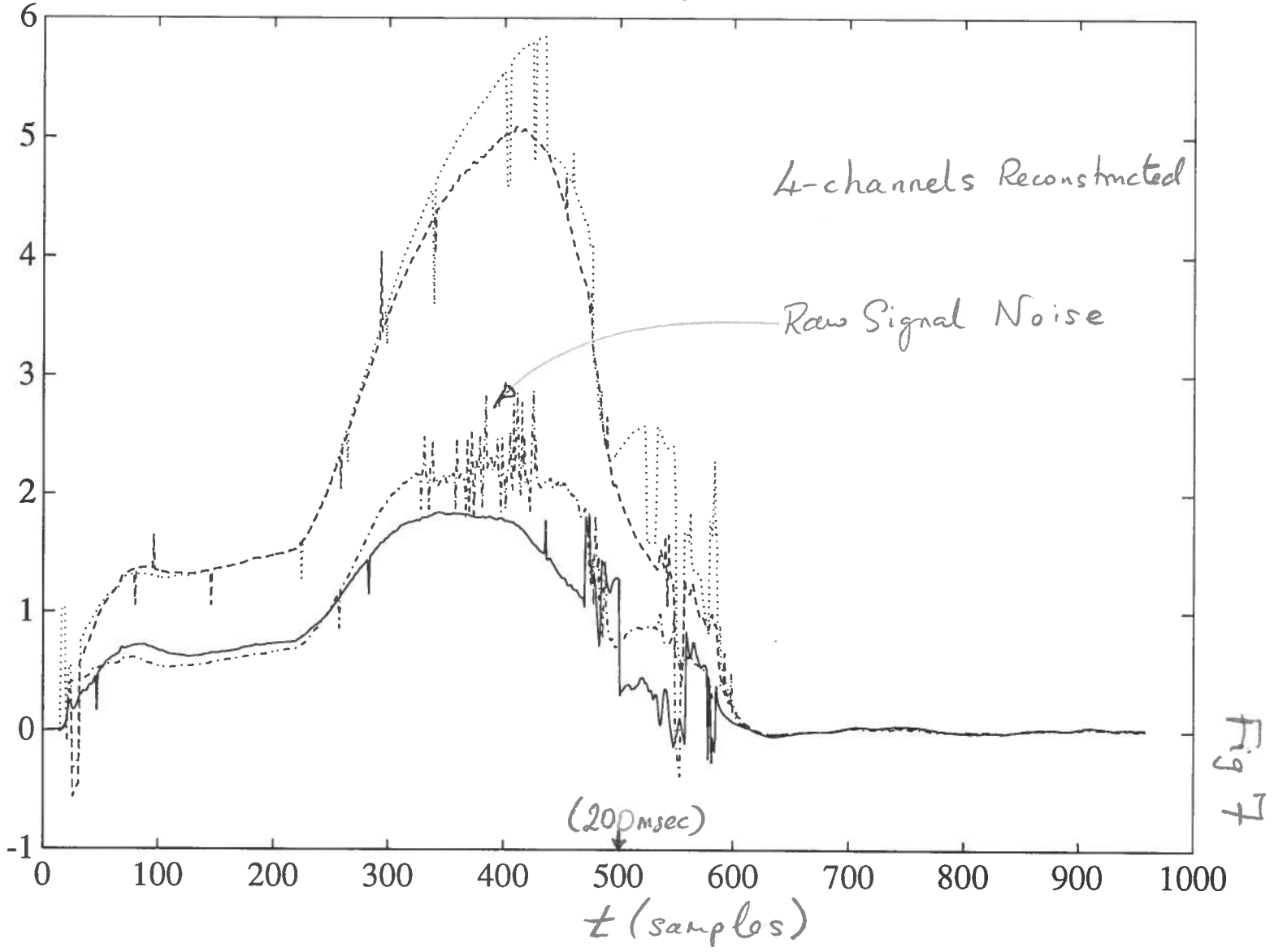
shot 38596 - fringe9 data
4-channels Reconstructed
Raw Signal Noise
(200msec)
t (samples)
6
5
4
3
2
1
0
-1
0
100
200
300
400
500
600
700
800
900
1000

Fig 7